View metadata, citation and similar papers at core.ac.uk

brought to you by CORE

provided by University of Dundee Online Publications

University of Dundee

Phase Velocity Dispersion Curve and Elastography Based on SAWs Induced by HIFU in Tissue Mimicking Phantoms

Zhou, Kanheng; Feng, Kairui; Li, Chunhi; Huang, Zhihong

Published in:
2018 IEEE International Ultrasonics Symposium, IUS 2018

DOI:
10.1109/ULTSYM.2018.8579997

Publication date:
2018

Document Version
Peer reviewed version

Link to publication in Discovery Research Portal

Citation for published version (APA):
Zhou, K., Feng, K., Li, C., & Huang, Z. (2018). Phase Velocity Dispersion Curve and Elastography Based on SAWs Induced by HIFU in Tissue Mimicking Phantoms. In 2018 IEEE International Ultrasonics Symposium, IUS 2018 (Vol. 2018-October). [8579997] IEEE Computer Society. https://doi.org/10.1109/ULTSYM.2018.8579997

General rights
Copyright and moral rights for the publications made accessible in Discovery Research Portal are retained by the authors and/or other copyright owners and it is a condition of accessing publications that users recognise and abide by the legal requirements associated with these rights.

- Users may download and print one copy of any publication from Discovery Research Portal for the purpose of private study or research.
- You may not further distribute the material or use it for any profit-making activity or commercial gain.
- You may freely distribute the URL identifying the publication in the public portal.

Take down policy
If you believe that this document breaches copyright please contact us providing details, and we will remove access to the work immediately and investigate your claim.

© 2019 IEEE. Personal use of this material is permitted. Permission from IEEE must be obtained for all other uses, in any current or future media, including reprinting/ republishing this material for advertising or promotional purposes, creating new collective works, for resale or redistribution to servers or lists, or reuse of any copyrighted component of this work in other works
Zhou, K, Feng, K, Li, C & Huang, Z 2018, Phase Velocity Dispersion Curve and Elastography Based on SAWs Induced by HIFU in Tissue Mimicking Phantoms. in 2018 IEEE International Ultrasonics Symposium, IUS 2018. vol. 2018-October, Kobe, Japan, 22/10/18. https://doi.org/10.1109/ULTSYM.2018.8579997

Phase velocity dispersion curve and elastography based on SAWs induced by HIFU in tissue mimicking phantoms

Kanheng Zhou
School of Science and Engineering
University of Dundee
Dundee, UK
k.y.zhou@dundee.ac.uk

Kairui Feng
School of Science and Engineering
University of Dundee
Dundee, UK
kfeng@dundee.ac.uk

Chunhi Li
School of Science and Engineering
University of Dundee
Dundee, UK
C.Li@dundee.ac.uk

Zhihong Huang
School of Science and Engineering
University of Dundee
line 4: Dundee, UK
z.y.huang@dundee.ac.uk

***Abstract*—Surface acoustic waves (SAWs) is a non-invasive and nondestructive method to detect elastic property of materials in industrial and medical field. Elastography derived from SAWs has been proved to be efficient for reconstructing the elasticity distribution map. Current SAWs elastography applied in tissues provides lower lateral resolution as the SAW impulse was detected in larger distance interval (millimeter level). Therefore, a new protocol to form elastography with higher lateral resolution was proposed in this paper. Phase sensitive optical coherence tomography (PhS-OCT) with high spatial resolution was employed to monitor SAWs impulse stimulated by HIFU transducer. Tissue-mimicking phantoms were tested in this experiment. SAWs dispersion curve was retrieved through processing wave signal with 2D fast Fourier transform based algorithm. Consequently, elastography of double layered phantom was constructed by combining SAWs dispersion curve and specific penetration depth. The results revealed feasibility for HIFU transducer acting as an ideal stimulation source for SAWs, and the elastography performed higher lateral resolution than that of other SAWs elastography techniques. Thus, the method raised in this paper showed a significant potential to be utilized in the clinical for skin disease diagnosis and assist monitoring treatment efficacy**

Keywords—HIFU, Surface acoustic waves, Optical Coherence Tomography, Elastography

I. INTRODUCTION

Physiological condition of tissues commonly were reflected by the mechanical properties such as Young's modulus indicating tissue stiffness [1][2]. Due to this property, skin diseases were mainly diagnosed in the way of palpation by trained and experimental dermal specialists. But this method lacks of consistency and quantitation because of the deviation of individuals. Therefore, it is highly demanding to emerge a quantitative assessment for the diagnosis of skin diseases.

One of current methods to access tissue elastic properties is surface acoustic waves elastography. It is a non-invasive, non-destructive technique to measure tissue elasticity by capturing the propagation of induced SAWs impulse on the superficial layer in tissues using laser vibrometer. The principle of SAWs elastography approach is employed the nature of dispersion. Rather than other elastography method where imaging depth is dominated by the range that imaging modality could reach, the penetration depth is only confined by the bandwidth of acquired SAWs signals. For current SAWs elastography technique, the method to track SAWs is dependent on laser vibrometer detector and the sampling spots have a few millimetre distance [3], leading produced elastography short of lateral resolution.

In this paper, we demonstrated an improving SAWs elastography method by combining Phase sensitive Optical Coherence Tomography (PhS-OCT) running at M-B mode to record the SAWs impulse stimulated by high intensity focused ultrasound (HIFU) transducer. M-B mode could ensure that the SAWs signal was sampled with higher lateral resolution than that by laser vibrometer. The SAWs impulse is narrow in time domain, meaning a wide bandwidth provided. Phase velocity analysis was achieved by an algorithm based on 2D fast Fourier transform, and SAWs dispersion curve deduced was utilized for the elastography reconstruction.

II. BACKGROUND OF SURFACE ACOUSTIC WAVE

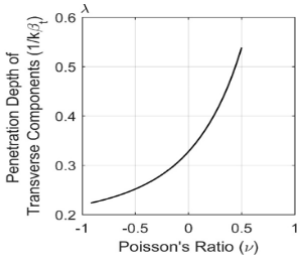

Fig. 1. The penetration depth (presenting in wavelength unit) of transverse component as the function of Poisson's ratio of materials (ranging from -1 to 0.5).

Technically, surface acoustic waves (namely Rayleigh waves), composing of longitudinal and transversal waves, are generated near free boundary (sample-air condition). The relationship between phase velocity (c_R) of SAWs and elasticity can be presented as follow [4][5]:

$$c_R \approx (0.87+1.12\nu) / (1+\nu) \times \sqrt{[E / 2\rho(1+\nu)]} \quad (1)$$

where E is the Young's modulus, ν indicates Poisson's ratio, and ρ is the density of material. Phase velocity under all the frequency is a constant when SAWs propagates in an isotropic homogeneous material. However, the phase velocity of different frequency components shows diverse while SAWs travel in a vertically heterogeneous material. SAWs with short wavelength (high frequency) mainly penetrate near the superficial layers while the long wavelength (low frequency) components primarily spread into the deeper layer. Although adjacent layers affect on the phase velocity of the middle layer, SAWs dispersion curve is still capable of reflecting the elasticity distribution of an anisotropic heterogeneous medium.

SAWs is regarded as superposition of longitudinal and transverse wave under the free-boundary condition, however the transverse component is dominant for the performance of SAWs. The maximum penetration depth z_{max} of SAWs for each frequency component could be estimated by an equation:

$$z_{max} = c_R / k\beta_t(\nu) \cdot f \quad (2)$$

where c_R is SAWs phase velocity, k is the wavenumber, f presents the frequency, ν denotes the Poisson ratio, and β_t were identified by

$$\beta_t = \sqrt{[1 - (c_R / c_t)^2]} \quad (3)$$

where c_t shows the velocity of transverse waves. The figure 1 shows the relationship between the penetration depth of transverse component ($1/k\beta_t$) [6].

III. MATERIALS AND METHODS

A. Tested sample

1% and 2% agar phantoms were used in this study to validate the availability to deduce the phase velocity dispersion curve. Double layers phantom then was produced for constructing the elastography. 2% and 1 % agar composed the double layer structure where 2% agar was placed on the top at 2 mm thickness.

B. HIFU transducer

A home-made High Intensity Focused Ultrasound (HIFU) transducer was used for generating SAWs. Before it was employed for stimulating the impulse signal, the output acoustic power and corresponding pressure field were calibrated by a radiation force balance, shown in figure 2. The output acoustic power raised up from 0.5 w to 10 w as the driving voltage fell into the range between 0.5 Vpp to 1.5 Vpp.

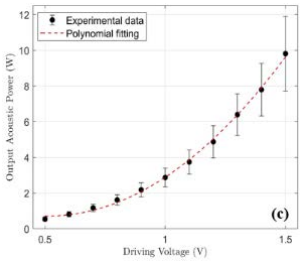

Fig. 2. The output acoustic power as the function of driving voltage.

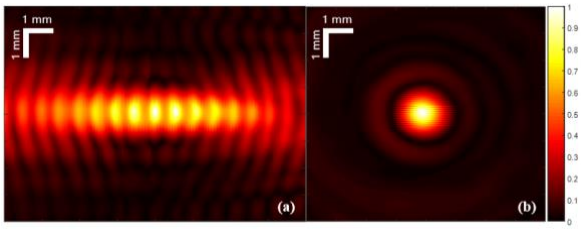

Fig. 3. Normalised pressure field distribution map of homemade HIFU transducer. (a) and (b) were respectively captured from axial and transverse axis, and both were in focus plane.

This customised HIFU transducer working at 1.488MHz frequency, has 20 mm aperture and 12.5 mm focal length. 2D normalised pressure field was mapping along the axial and lateral axis cross the focal point, presented in figure 3 (a-b), which was detected through a hydrophone with 500 μm diameter. The geometry of focal zone was 7.7 × 1.1 mm (axial × radial) defined by full-width-half-maximum (FWHM), which provided sufficient length at axial axis to cover the imaging depth of PhS-OCT system (3 mm maximum).

C. Phase sensitive Optical Coherence Tomography (PhS-OCT)

In this study, PhS-OCT system based on spectral domain was utilised for tracking SAWs impulse generated by HIFU transducer. The entire configuration of this optical system is composed of a broadband laser as light source, a 90/10 beam splitter, a 2D galvo scanning system, a spectrometer camera and reference/sample arms. The broadband laser source has 1310 nm central wavelength, 83 nm bandwidth and 10 mW power. The spectrometer is a line scan CCD operating at 91.2KHz frequency and 6.96 μs exposure time. The light beam is emitted from the source and consequently is split by beam splitter, where part of beam is lead into sample arm while the rest go into the reference arm. The sample arm is responsible for leading the light beam into the sample surface, from which backscattered light is interfered with that reflecting from the reference mirror in a circulator. The resulted interfered light beam is recorded by the line CCD camera. This spectral domain OCT system produce an axial resolution of 8.6 μm and transverse resolution of 14.2 μm. The axial displacement at a certain location $u_z(x, z, t)$ between the adjacent two frames was derived from the phase difference $\Delta\varphi(x, z, \Delta t)$. The relationship between both pamareters is writen as：

$$u_z(x, z, t) = \Delta\varphi(x, z, \Delta t) * \lambda / 4\pi n \quad (4)$$

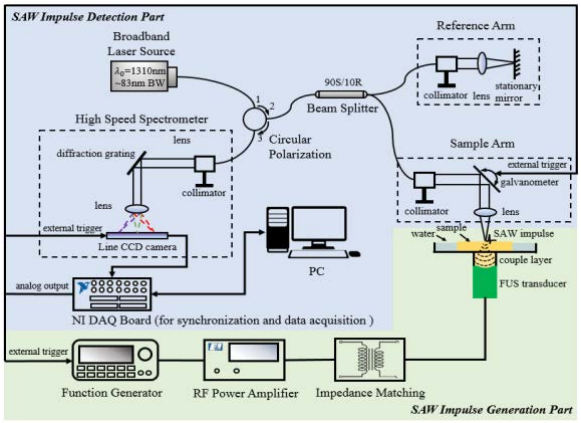

Fig. 4. The entire experimental setup for generating SAWs could be classified into two parts: (1) the generation of SAWs impulse and (2) the detection of SAWs.

where λ is the central wavelength (1310 nm) of laser source, n denotes the refractive index of the sample. The minimum phase difference that could be detected by this system is 0.06 rad.

D. *The experimental configuration of SAWs elastography*

The entire experimental setup could be classified into two parts: (1) the generation of SAWs impulse and (2) the detection of SAWs. For applying the load induced by HIFU transducer on material surface, the transducer was places beneath the sample. The distance between the surface of phantoms and transducer equals to the focused length, ensuring that the ultrasound load was irradiated on the air-sample free boundary to generate SAWs. The gap between the transducer and phantoms was filled by homogeneous agar phantom (2%), acting as the medium for facilitating the spread of ultrasound. The ultrasound was triggered by functional generator with sine-wave at 1.4 Vpp, 1.488MHz and 100 cycles per pulse in burst mode. RF power amplifier was connected between the functional generator and HIFU transducer to strengthen the signal. In addition, a 50 Ω impedance matching circuit was inserted between RF power amplifier and HIFU transducer.

E. *Phase velocity dispersion curve and Elastography reconstruction*

The principle of rebuilding the elastography was the SAWs dispersion curve. 2D fast Fourier transform is the key to derive the phase velocity in the algorithm. Before applying 2D fast Fourier transform, a spatial-temporal slice displaying SAWs propagating in the material surface was abstracted and unwrapped to obtain correct phase information. 2D fast Fourier transform convert spatial-temporal image from space-time domain into wavenumber-frequency domain (*k-f* domain). According to the equation [7]:

$$C_R(f) = f / k_L \tag{5}$$

Where f is the frequency, $C_R(f)$ represents the phase velocity of certain frequency, k_L denotes the wavenumber, the phase velocity dispersion curve could be deduced by selecting the velocites with maximal intensity at each frequency component. The cut-off frequency was chosen at the point where the intensity is less than the maximum -30 dB.

Final procedure for proceeding data was transforming the phase velocity dispersion curve into Elastography image. Through combining the phase dispersion curve and corresponding maximum penetration depth estimated from equation 2, the phase velocity map could be calculated, followed by converting it into elasticity distribution map by plugging the phase velocity into equation 1. Although the elastography represented the elastic property at the range from wave source to the far field, the valid zone is defined within the far field and the near field which was defined from wave source to 1.5 mm away was removed. The reason was that the superposition of other ultrasound acoustic waves and other frequency components of SAWs might affected the elasticity analysis.

IV. Results and Discussion

A. *Results*

Figure 5 (a-c) illustrated procedures from initial spatial-temporal slice to phase velocity dispersion curve. The original spatial-temporal slice before unwrap shown in figure 5(a) indicated that SAWs impulse simulated by HIFU transducer propagated from irradiated point to 5 mm away. And the frequency-wavenumber domain deduced from the time-distance domain was shown in figure 5 (b). The phase velocity dispersion curve within cut-off frequency range was shown in figure 5 (c), The phase velocity fell into the frequency scope between 1 KHz to 4 KHz. According to the equation 2, the penetration depth fell into 0.53mm to 2.21 mm from surface in the phantom. As 1 % phantom was a homogeneous material, it is clear to see that the phase velocity under each frequency component almost remained constant. The mean SAWs velocities travelling in 1 % and 2 % phantoms were deduced to be ~4 m/s and ~8.1 m/s respectively.

Figure 6 (a) displayed the phase velocity dispersion curve in multi-layered phantom where the top was 2% agar in ~2mm thickness and 1% agar was the basement. As described in the part of Background of SAWs, the phenomenon of dispersion occurs within the vertically heterogeneous material. The higher frequency components mainly spread on the facial layer (2% agar) while the lower frequency component propagated in 1% agar layer. Thus, the velocity at higher frequency part was higher than that of lower frequency components in the dispersion curve.

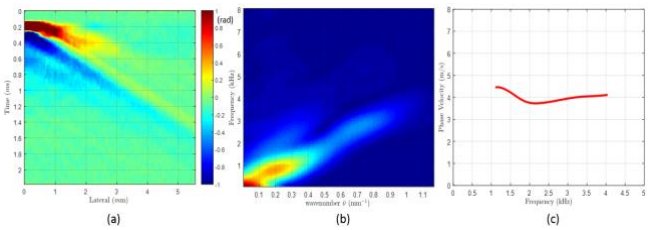

Fig. 5. (a) Original spatial-temporal slice from the surface of tissue-mimicking phantom. (b) wavenumber-frequency domain image derived from fig 5 (a) using 2D Fourier transform. (c) SAW dispersion curve within cut-off frequencies (1.1 KHz to 4.05KHz).

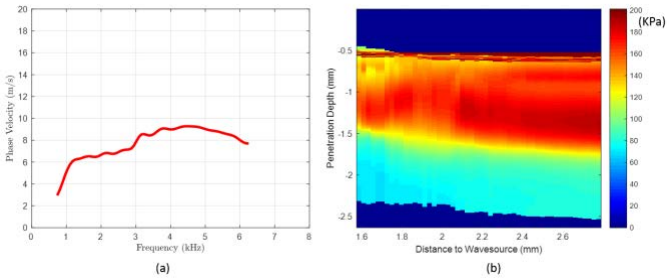

Fig. 6. (a) SAWs dispersion curve within cut-off frequencies (0.8 KHz to 6.3 KHz) in double layered phantom. (b) Elastography of doubled layered phantom where 2% agar was on the top and 1% agar was basement.

Figure 6 (b) represented the elastography estimated from the equation 1 and phase velocity map derived through combining dispersion curve and penetration depth information. The vertical heterogeneous attribution of multi-layered structure was performed in the elastography. 2% agar phantom with 2 mm thickness as top layer has the Young's modulus ~200Kpa, and the Young's modulus of 1% agar as a basement was ~80 KPa. Both of these two results agreed well with our previous works [8][9].

B. Discussion

For isotropic homogeneous material, we derived the phase velocity dispersion curve for 1% and 2% agar phantom and the velocities were 4 m/s and 8 m/s respectively, corresponding to the Young's modulus of ~50KPa and ~200 KPa. In the elastography image, the Young's modulus of 2% agar phantom on the top matched the value coming from homogeneous 2% agar phantom. However, the stiffness of 1% agar as basement seemed to be greater than that of homogeneous 1% agar. The possible factor for this deviation was the influence caused by the top layer. As mentioned in the part of Background of SAWs, the adjacent layers impact the phase velocity for middle layer, and this definitely made the Young's modulus of one single layer in the skin biased from the real value. Thus, it is the future work to correct the Young's modulus for each layer on the vertically heterogeneous material, by demodulating the dispersion curve from the composed phase velocity dispersion curve.

The elastography produced in this study just demonstrated the elasticity value for part of facial layer. The information from the surface to the depth (~0.5 mm) was missed. The potential factor is that the narrow bandwidth of SAWs impulse signal generated. The maximum frequency component determine the minimum penetration depth. In this experiment, the highest frequency 6 KHz restricted the top layer that can be derived was 0.4 mm away from sample surface. Shear wave elastography should be an ideal method to supply missing superficial zone in SAWs elastography.

In this paper, the devices for SAWs impulse generating and tracking were installed on both sides of phantoms. Besides, extra agar phantom was inserted between transducer head and sample. This design restricted the feasibility in in-vivo clinical applications. Recently, new-emerged air-coupled focused ultrasound transducer has been applied for inducing mechanical waves in non-contact way [10]. Predictably, SAWs elastography using dispersion curve would be able to develop for in-vivo clinical field through bringing in non-contact ultrasound transducer.

V. Conclusion

This paper presented an improved SAWs elastography method with higher lateral resolution, by combining HIFU transducer for stimulating waves and PhS-OCT system for recording waves. Phase velocity dispersion curve, which was analyzed by 2D Fast Fourier transform, was deduced to achieve the elastography. The Young's modulus calculating from this method for phantoms with different concentrations was accordant with the reference value. The proposed method reveals the potential to provide elastography with higher lateral resolution compared to current SAWs elastography technique. Besides, it is predicted that the multi-layered structure of skin could be distinguished using this advanced approach. In conclusion, the HIFU transducer can be an ideal source to generate SAWs and the SAWs elastography method presented in this paper performed significant potential for the skin disease diagnosis and treatment monitor in the clinical field.

References

[1] Gennisson JL, Baldeweck T, Tanter M, Catheline S, Fink M, Sandrin L, Cornillon C, Querleux B, "Assessment of elastic parameters of human skin using dynamic elastography," IEEE transactions on ultrasonics ferroelectrics and frequency control, 51(8):980-9 (2004).

[2] Raveh Tilleman T, Tilleman MM, Neumann HA, "The elastic properties of cancerous skin: Poisson's ratio and Young's modulus," Optimization of Incisions in Cutaneous Surgery including Mohs' Micrographic Surgery, 105 (2004).

[3] Li C, Guan G, Zhang F, Nabi G, Wang RK, Huang Z. "Laser induced surface acoustic wave combined with phase sensitive optical coherence tomography for superficial tissue characterization: a solution for practical application" Biomedical optics express, 5(5):1403-18 (2014).

[4] Neubrand, A, Hess, P. "Laser generation and detection of surface acoustic waves: elastic properties of surface layers," J. Appl. Phys, 71, 227–238 (1992).

[5] Schneider, D, Schwarz, T. A. "Photoacoustic method for characterising thin films," Surf. Coat. Tech., 191, 136–146 (1997).

[6] Maradudin A. A. "Surface acoustic waves on real surfaces," Physics of Phonons, 82-147 (1987).

[7] Maksuti E, Widman E, Larsson D, et al. "Arterial Stiffness Estimation by Shear Wave Elastography: Validation in Phantoms with Mechanical Testing," Ultrasound in medicine & biology, 42(1): 308-321(2016).

[8] C. Li, G. Guan, S. Li, Z. Huang, and R. K. Wang, "Evaluating elastic properties of heterogeneous soft tissue by surface acoustic waves detected by phase-sensitive optical coherence tomography," J. Biomed. Opt., 17(5): 057002 (2012).

[9] C. Li, G. Guan, R. Reif, Z. Huang, and R. K. Wang, "Determining elastic properties of skin by measuring surface waves from an impulse mechanical stimulus using phase-sensitive optical coherence tomography, " J. R. Soc. Interface, 9(70):831–841 (2012).

[10] Ambroziński Ł, Pelivanov I, Song S, Yoon SJ, Li D, Gao L, Shen TT, Wang RK, O'Donnell M. "Air-coupled acoustic radiation force for non-contact generation of broadband mechanical waves in soft media," Applied physics letters, 109(4):043701 (2016).